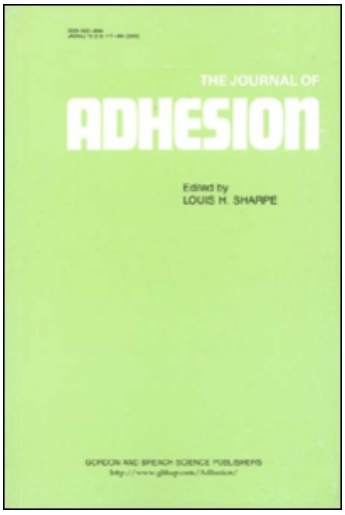

The Journal of Adhesion

Publication details, including instructions for authors and subscription information:
http://www.informaworld.com/smpp/title~content=t713453635

Adhesion Failure in the Stick-Slip Regime: Optical and AFM Characterizations and Mechanical Analysis

G. Ryschenkow[a]; H. Arribart[a]
[a] Laboratoire C. N. R. S./Saint-Gobain "Surface du Verre et Interfaces", Aubervilliers, France

To cite this Article Ryschenkow, G. and Arribart, H.(1996) 'Adhesion Failure in the Stick-Slip Regime: Optical and AFM Characterizations and Mechanical Analysis', The Journal of Adhesion, 58: 1, 143 — 161
To link to this Article: DOI: 10.1080/00218469608014403
URL: http://dx.doi.org/10.1080/00218469608014403

J. Adhesion, 1996, Vol. 58, pp. 143–161
Reprints available directly from the publisher
Photocopying permitted by license only

Adhesion Failure in the Stick-Slip Regime: Optical and AFM Characterizations and Mechanical Analysis*

G. RYSCHENKOW and H. ARRIBART

Laboratoire C. N. R. S./Saint-Gobain "Surface du Verre et Interfaces", BP 135, F-93303 Aubervilliers, France

(Received August 11, 1995; in final form Feburary 27, 1996)

Peeling experiments are sometimes perturbed by the so-called "stick-slip" regime of failure, where the measured peeling force evolves in a jerky way. Approached here as a multileveled instability, this regime was intentionally provoked at low speed and high temperature tests. Using optical and Atomic Force Microscope (AFM) techniques, careful examinations of the failure surfaces exhibit reproducible, somehow ordered, polymeric residues, the geometry of which depends on the peeling temperature. The structures observed at the microscopic scale are discussed in terms of void formation, as in the crazing mechanism, in relation to the bifurcative cellular pattern appearing at the macroscopic scale. An interpretation for always finding the locus of failure near the interface is given.

KEY WORDS: Adhesion; adhesive failure; atomic force microscope; crazes; glass; instabilities; interface; peeling test; polyurethane; stick-slip.

INTRODUCTION

The adhesion of elastomer/substrate joints is generally studied by using the peeling test. It is well known that this test does not give a direct measurement of the intrinsic adhesion energy, G_o, between the two components, but delivers a work of detachment, G, which depends on experimental conditions: velocity, v, of the crack propagtion, ambient temperature, T, and the nature of the environmental medium.

In many cases, it has been experimentally proved that this measured energy is proportional to the interfacial adhesion energy, G_0,[1] with an amplificative factor, Φ, from 1 to 10^4, that can be scaled by the WLF shift factor a_T of the polymer:[1-5]

$$G(v) = G_0 \Phi(a_T v) \tag{1}$$

This dependence demonstrates the importance of viscoelastic losses inside the polymer during the test, but how they act is difficult to model because several

* One of a Collection of papers honoring Jacques Schultz, the recipient in February 1995 of the *The Adhesion Society Award for Excellence in Adhesion Science, Sponsored by 3M.*

mechanisms can operate simultaneously (reptation, disentanglement, chain suction, chain scission, etc.) and, also, at different scales: from the individual molecule to the collective rheological behavior.

Moreover, depending on the main quantity $a_T v$, different modes of failure are observed, from purely adhesive (or interfacial), to purely cohesive. A transition from adhesive to cohesive failure, driven by the rheology of the elastomer, must occur when the temperature is increased or the peeling rate is reduced[3,6]. We have shown in previous studies that, for some systems, such as the glass/polyesterurethane one used in the present study, the failure is, in fact, never purely interfacial[7,8]. A very thin layer of polymeric materials remains on the glass substrate. This was called the quasi-interfacial failure. In the same work, Atomic Force Microscopy (AFM) observations of the glass surface after failure revealed a non-homogeneous surface composed of microscopic islands of polymer residues, organized in rather regular bumps of several tens nanometers height and about 100 nm in diameter (see Fig. 2b in Ref. 7). Such a topography can be understood as polymeric prints reminiscent of the polymer distribution just before the complete failure occurred, and suggests a *fibrillation mechanism*. This set of observations confirms that deformation and flow occur at different scales during a peeling test.

A last fact about peeling, well known by experimentalists in the field, is the possible recording of a markedly unsteady force as a function of time. Considering Equation (1), this means that the instantaneous velocity of the crack propagation, v, is not constant, even for a fixed peeling rate, V. Regular periodic oscillations as well as jerky and erratic behaviors can be observed. These different regimes occur in certain ranges of imposed temperature and peeling rate. They correspond to situations where the system hesitates between the two modes of failure and sequentially jumps from one to the other in an either periodic or chaotic manner. This is the so-called "stick-slip" regime[9].

In this paper, based on the optical and AFM observations of the surfaces resulting from the propagation of the peeling front, we try to show that the stick-slip regime i) can be somewhat demystified and ii) can bring new insights to the overall understanding of the behavior of an adhesive joint subjected to high mechanical stresses.

The paper begins with a recall of the admitted explanation of the stick-slip regime[10-13]. Then, we present a study at the macroscopic scale which shows that it is not satisfactory to think about peeling as a one-dimensional experiment. In fact, bifurcation of the failure front can occur, leading to non-homogeneous stresses along the front line. A complete explanation of these phenomena would imply the use of recent concepts developed in non-linear physics. We only show here that the behavior of the system is non-deterministic. Then, the structure of the polymer residues on the glass substrate observed at the mesoscale is presented. It allows for a qualitative description of the deformation and flow of polymeric matter ahead of the failure front, similar to the crazing mechanism well-known in polymer physics and, we conclude, to the formation of voids, as suggested by Gent and Petrich,[3] and theoretically considered by Kaelble[14]. At last, we discuss the relation between phenomena occuring at the macroscopic and at the mesoscopic scales.

THE STICK-SLIP REGIME

Following the arguments of Maugis and Barquins,[10] this macroscopically unstable regime of rupture can be understood as the result of the existence of two rising branches in the $G(v)$ curve separated by a decreasing one (see Fig. 1). If the imposed machine speed, V, is chosen in the unstable range, the system successively accelerates, in order to peel at lower energy and higher speed ("slip" stage, point A), so in the *adhesive* mode. Because the elastic energy stored in the peeled strip is instantaneously released, it then decelerates towards a very low velocity (point B) and low peel strength, G_{min}. From that state, the peeled strip is stretched again, then the crack velocity slowly increases following the $G(v)$ curve and the failure becomes *cohesive* ("stick" stage) until a critical high peel strength, G_{max}, is reached (point C) where the velocity is too low compared with the macroscopic imposed speed. Then the system is forced to return to the high velocity regime (point A) and the cycle is completed.

The experimental force recording, $F(t)$, is thus saw-tooth shaped as illustrated in Figure 3 (the strain energy release rate, $G(t)$, is just equal to force, $F(t)$, divided by the sample width, b). During one period of oscillation, this curve does not represent either the $G(v)$ function or the $G(x)$ one (x is the crack front abscissa) because, precisely, the crack front velocity is never constant in that regime of failure. As pointed out by Maugis,[13] the system spends most of the time in the cohesive mode, but the higher peeled distance is traced during the short adhesive mode. In fact, the force recording is dominated by the alternation of stretching and relaxation of the peeled strip. Further information could be obtained from the critical values, G_{min} and G_{max}, which are somehow related to the threshold adhesion energy and to the

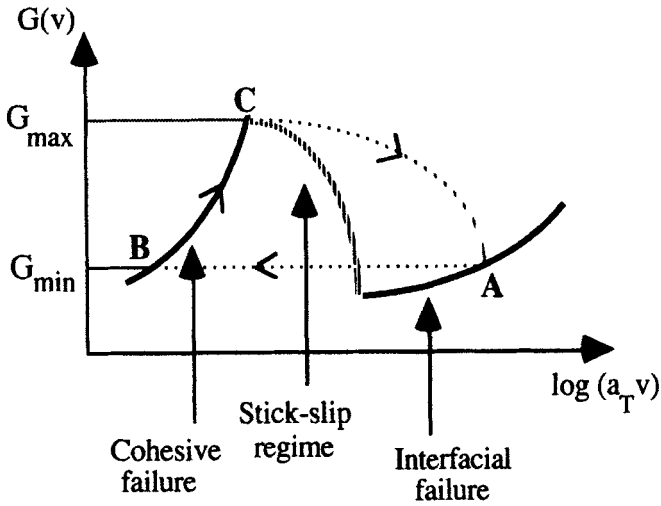

FIGURE 1 Principial peeling master curve representing steady state regimes (full line) and unstable regimes (dashed line). When the experimental conditions (V, T) are chosen in the unstable range, the system evolves along the dotted curve.

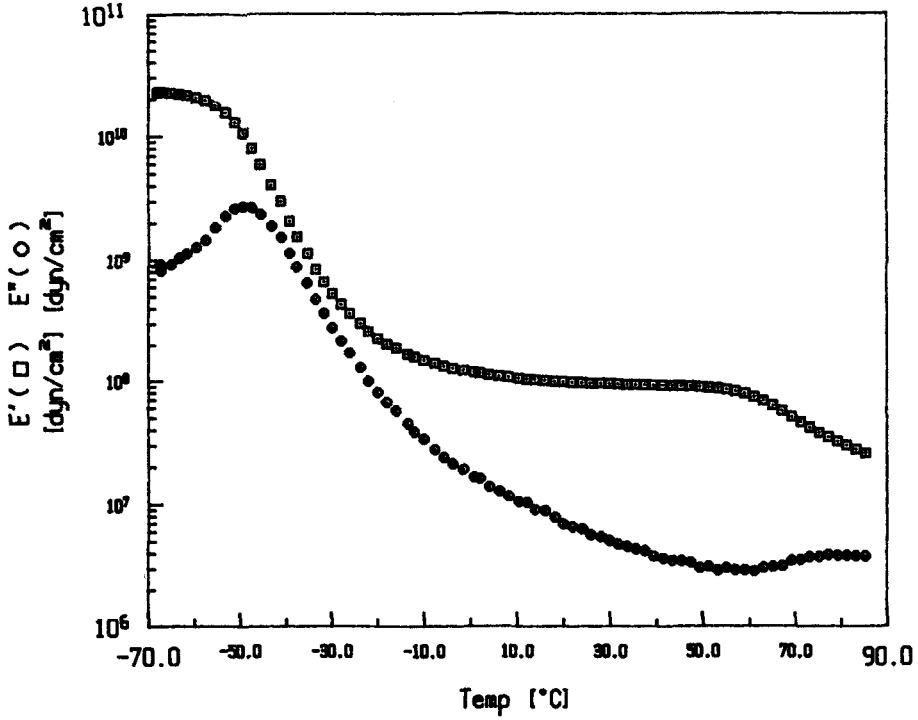

FIGURE 2 Dynamic measurements (DMTA) of the storage (E') and loss (E'') modulii of the Polyurethane at 1 Hz for the temperature range of interest.

maximum stress sustainable in the cohesive mode. However, this requires a better understanding of the stability of this regime. We show in the following that significant insights for that matter can be deduced from the careful observation of the peeled surfaces.

MACROMECHANICS OF THE STICK-SLIP

1. Experimental Observations

The studied system, already described in this Journal,[7] is composed of a backed polyester urethane (PU) film (thickness ≈ 0.8 mm) synthetized by SNPE, France, joined by hot-pressing to flat float-glass samples provided by Saint-Gobain Vitrage France. The adhesion strength is measured by the 90°-peeling test using an Instron machine at its lowest speeds, V(0.5–1 mm/mn), and a temperature regulated chamber at different temperatures, from 20°C to 65°C. The polymer is a H_{12} MDI copolymer,[15] composed of "soft" polyester caprolactone segments and "hard" diisocyanate segments. Its rheological properties characterized by DMTA are reported in Figure 2. The glass transition temperature is around -48°C and the

rubbery plateau extends from about 0°C to 50°C. From this last temperature, the elastic modulus, E', starts to fall regularly, before the terminal zone (beyond 110°C, not shown in the figure) where the polymer becomes completely liquid. This fall, beginning at 50°C, is understood as a melting of the physical crosslinks composed of hydrogen-bonded crystalline clusters of hard segments,[15] giving rise to liquid-like properties at much longer distances than at the rubbery plateau. In that region, the behavior becomes more dissipative than at room temperature and it must be pointed that it is essentially in this region of temperature that we observe the stick-slip mode of rupture.

Before entering into the full description of the experimental results, it is worth noting that the force oscillations observed during the stick-slip process are not due to an artifact caused by the weave of the backing. For the two very different backings used, a natural cotton cloth and a strong linen one, the spatially measured periodicities of the stick-slip process, around 3 ± 1 mm, do not fit to the weave periodicities, respectively 0.8 and 0.5 mm, for the two cloths (the last one is visible in Fig. 7).

As for many other investigators,[9-12] we observe different degrees of regularity in the recordings of the peel strength *versus* time. The amplitude, $G_{max} - G_{min}$, and the periodicity of the oscillations may vary, but it is important to distinguish the external causes (local pollution of the interface, irregularities in the geometry, etc.) from the intrinsic ones. For example, it has been observed that, for increasing imposed speeds, the recordings become chaotic,[10,12] a phenomenon generally encountered in dissipative dynamic systems.[13,16] A more-to-the-point example can be seen in Figure 3. The first small drop in the peel force may appear as an accident but, as we will see later on, it is not fortuitous. The occurrence of this event strongly depends on the temperature, T, of the test.

In order to understand the meaning of the recorded force variations, we systematically observed, using a reflection optical microscope, the surfaces of both adherends after the peel test, as sketched in Figure 4. The PU debonded surface corresponding to the force recording of Figure 3 is shown in Figure 5. It presents a succession of rugged stripes roughly perpendicular to the peeling direction separated by larger flat zones. The rugged stripes correspond to an increase in polymer height of about 100–200 μm relatively to the flat zones. These stripes result from plastic deformation and are formed during the long period of time when the peeling force is rising to the maximum (stick stage), whereas the large flat zones in between appear during the short period of time when the force drops to the minimum (slip stage). The optical analysis of the peeled glass surface confirms the general principles given in the preceding section. Opposite to the rugged stripes, the glass substrate is covered with PU residues of micrometric thickness. This means that the failure is cohesive even at the optical scale (an illustration is given in Figure 6 for a higher peeling temperature in which case the residues are clearly visible). At variance, opposite to the flat zones, the failure appears interfacial at this scale (a more detailed AFM analysis will be presented in the next section).

In Figure 5, as shown by an arrow, the first rugged stripe is divided into two branches. The crack front does not propagate in-phase all along, but only a part of its slips in advance. This phenomenon is called spatial bifurcation. The next slip

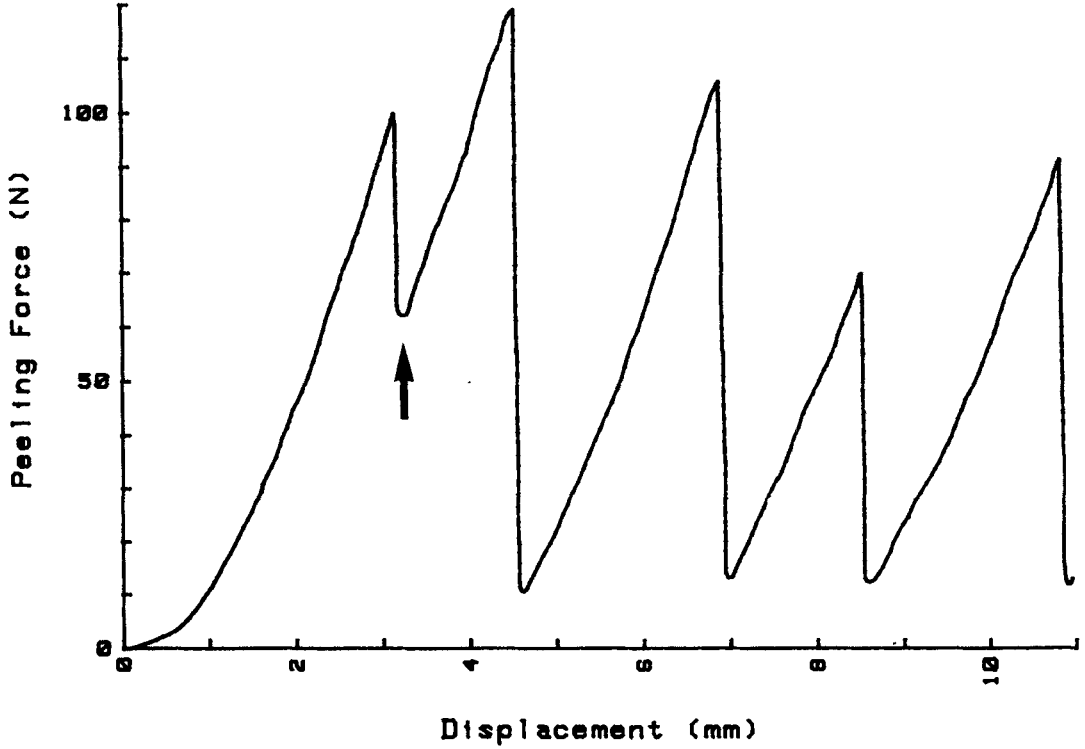

FIGURE 3 Experimental recording of the peeling force as a function of time or displacement. Experimental conditions: imposed machine speed $V = 0.5$ mm/mn, $T = 50°C$, sample width $b = 12$ mm. The polymer strip is backed with a cotton cloth. Drops of the force are correlated with slip stages where the crack speed, v, is much higher than V (see text). The arrow shows a frustrated force drop.

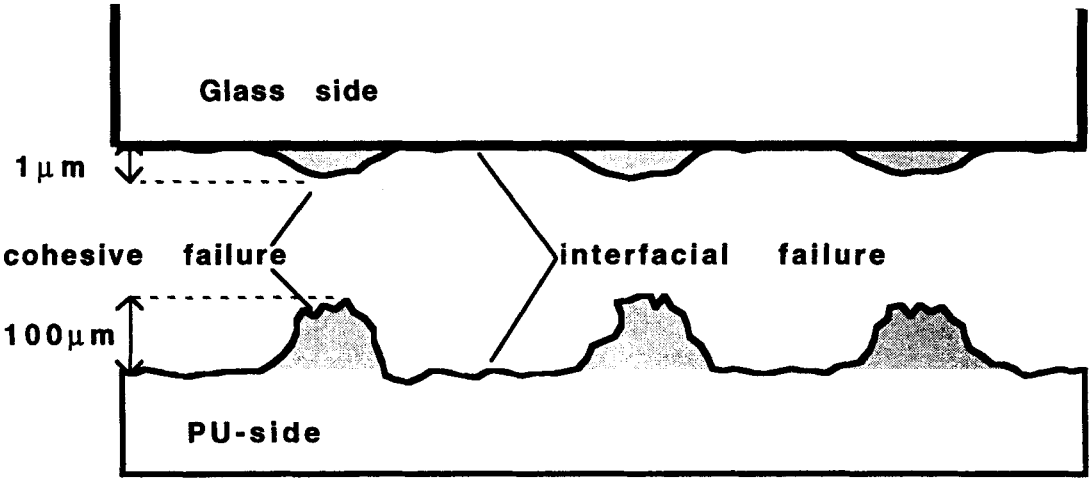

FIGURE 4 Cross-sectional sketch parallel to the peeling direction of the corresponding sides of the adherends after rupture.

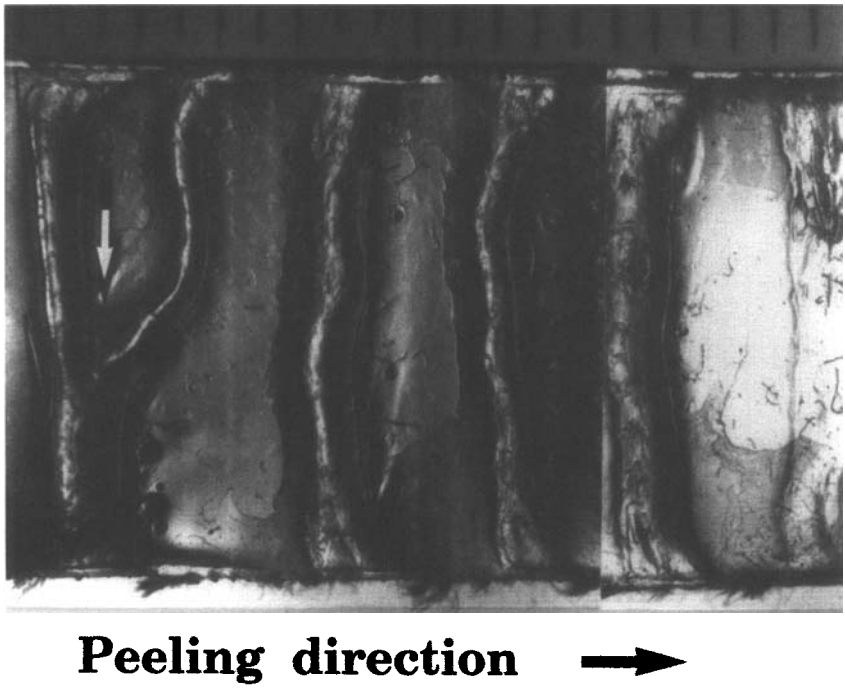

FIGURE 5 Optical photograph of the peeled polymer strip which corresponds to the force recordings of Figure 3. The bifurcation marked by an arrow is related to the frustrated force drop of Figure 3. Scale in millimeters.

event restores a roughly straight front. This unique bifurcation is clearly visible on the corresponding peel force recording as the frustrated drop, mentioned before and shown by the arrow in Figure 3, where the regular minimum is not reached.

At lower temperatures, we observe a much more frequent occurrence of these bifurcations. On the same test piece, we performed four different consecutive isothermal peelings (equal increment $\Delta T = 5°C$) separated by the time duration necessary for thermalisation. The PU side peeled at 40°C (left of the Fig. 7) reveals so many bifurcations that the surface appears divided into cells, the interior of which corresponds to the fast interfacial failure (slip event). It is important to notice that the areas, ΔS_i, of these cells are not constant and seem to vary randomly. More precisely, if b_i denotes the width of cell i, and Δx_i its length, i.e. the slip distance of the i-th event, it appears that the variations of ΔS_i are essentially due to the fluctuations of b_i, the slip distance Δx_i being roughly constant, around 2 mm.

These observations have their counterpart in the recorded peeling force of Figure 8. To the fifteen numbered cells exactly correspond fifteen drops of the force. Moreover, for each event i, the measured amplitude, ΔF_i, of the force drop is proportional to the measured corresponding cell area, ΔS_i, as shown in Figure 9. The same analysis applies to the three other consecutive temperatures (see Fig. 7, left to right), the coefficient of proportionality remaining the same (see Fig. 9). But for these four

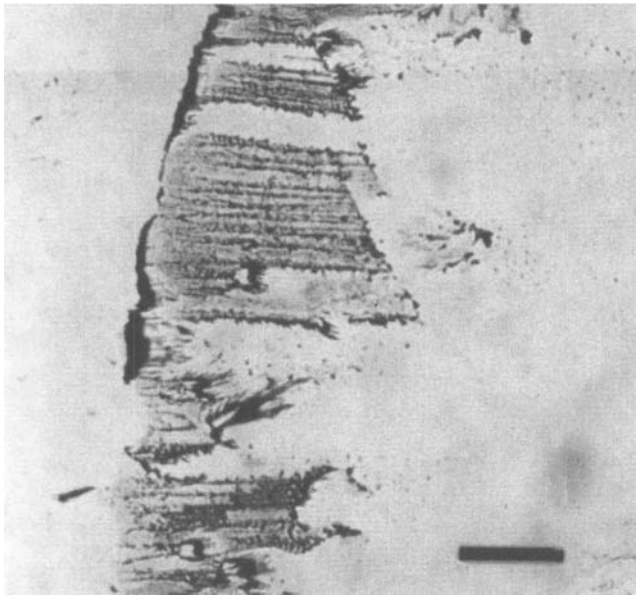

Peeling direction →

FIGURE 6 Optical micrograph of the peeled glass substrate showing polymer residues resulting from the stick stage (cohesive mode of failure). Experimental conditions: $T = 65°C$ and $V = 0.5$ mm/mn. These residues are organized in regularly festooned walls parallel to the peeling direction. The scale bar represents 100 μm.

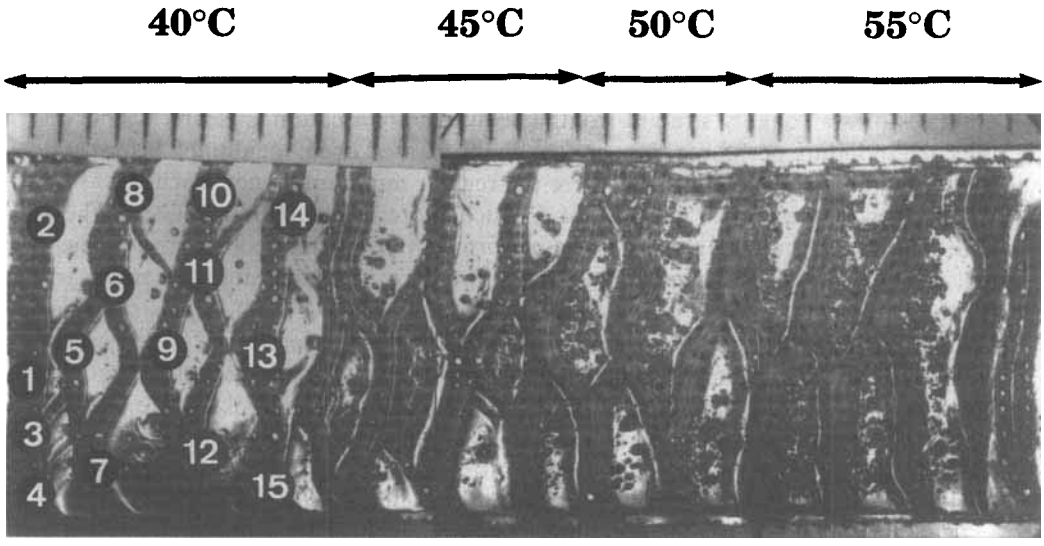

Peeling direction →

FIGURE 7 Optical photograph of the peeled polymer strip after peelings at four successive temperatures from 40°C to 55°C, from the left to the right. The left side of each slip sequence cell is numbered for the 40°C peeling. The polymer strip is backed with a strong linen cloth. $V = 0.5$ mm/mn. Scale in millimeters.

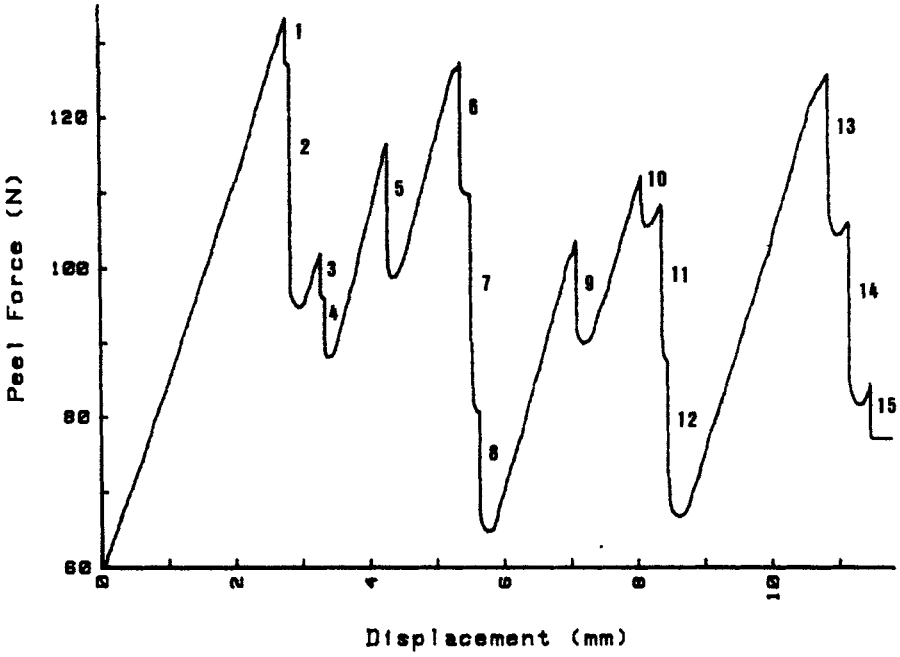

FIGURE 8 Recording of the peeling force during the isothermal peeling at 40°C corresponding to the left side of Figure 7. Each drop of the force is numbered in correspondence with each slip event detected on the photograph of Figure 7.

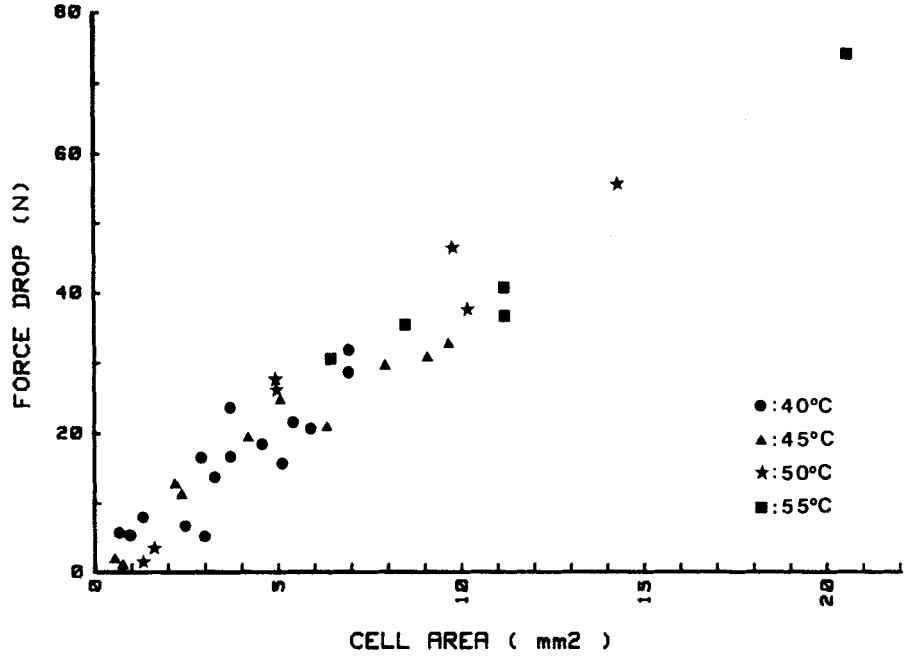

FIGURE 9 Plot of the amplitude, ΔF_i, of the drops of the recorded peeling force *versus* the corresponding area, ΔS_i, of the cells of Figure 7, for the four temperatures. For the 40°C points, the ΔF_i values are those measured on Figure 8.

different test temperatures the qualitative observations are conspicuously different: when the temperature is raised, the number of bifurcations decreases, the crack front straightens (in correlation with a better regularity in the force oscillations) and the interfacial domains tend to occupy all the sample width. This leads us to define a macroscopic transverse coherence length, Ξ, which increases with temperature.

This last feature is apparently difficult to reconcile with the fact that, at higher T, the polymer is less cohesive, but the later AFM observations will bring some insights into this apparent paradox.

2. Mechanical Analysis

We propose now an explanation for the two main results described above, namely the jerky behavior of the peeling force and the linear relation between the peel force drops and the corresponding slip cell areas. We model the rheological behavior of the system as follows. The major part of the mechanical displacement is ensured during the stick stage by the elasticity of the peeled strip and the viscous effects in the polymeric film. But during the very short slip event the behavior is only elastic and we may disregard the dashpot element. Then, on the basis of the preceding observations, we divide the advancing front of total width, b, into elementary uncorrelated parts of widths b_i (equivalent to Ξ). As we shall see in the following, this unpredictable length chosen by the system cannot be mechanically determined. This means that its value is very sensitive to small local fluctuations of the joint properties, even if its general tendency is to increase with temperature. We can, thus, represent the whole system by the mechanical model represented in Figure 10, where the conventional symbols are used. The solid friction element (anti-slip pad) simulates the adhesion resistance to peeling by the simplified two energy level diagram of stress *versus* velocity represented in Figure 11. The static force, $b_i\Gamma_i^S$, is equivalent to the maximum peeling force in the cohesive mode (*i.e.* at low speed), and the dynamic one, $b_i\Gamma_i^D$, to the minimum one (*i.e.* at high speed). In that case, when the total peeling force rises from zero, the weaker pad, say j, will first slip over the distane Δx_j, relaxing by that event the whole system stress state and thus delaying the same event for the other i-elements associated with widths b_i. Neglecting inertial and viscous effects, the corresponding force drop can be written as:

$$\Delta F_j = b_j(\Gamma_j^s - \Gamma_j^D) \tag{2}$$

Besides, simple evaluations of the elastic forces sustained by the peeled strip before (F_b) and after (F_a) the slip event give:

$$F_b = Ebw[L(t) - L_0]/L_0 = Ebw\varepsilon \tag{3}$$

$$F_a = Ebw[L(t) - L_0 - \Delta x_j b_j/b]/[L_0 + \Delta x_j b_j/b] \tag{4}$$

where E is the Young's modulus of the peeled strip (PU + packing), w its width, L_0 its initial length, $L(t)$ its length at the event time t and ε its tensile strain. With the

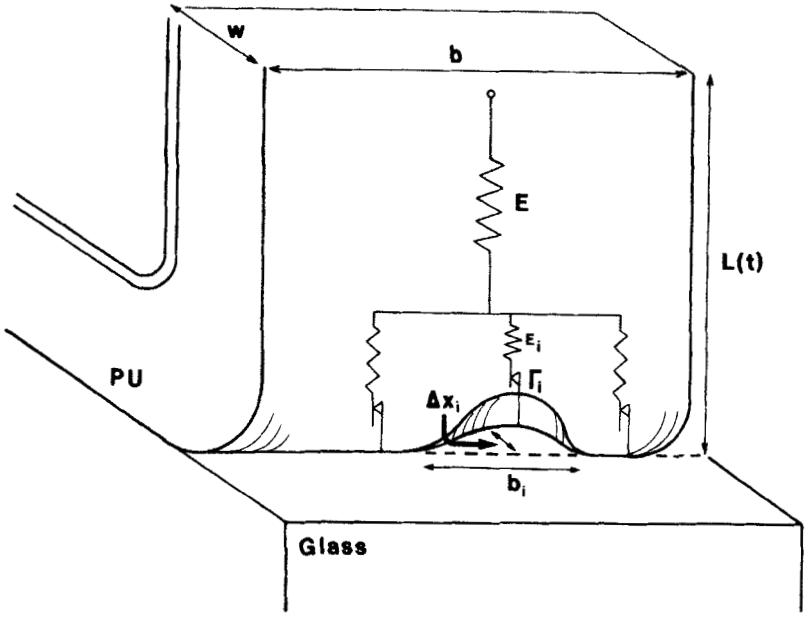

FIGURE 10 Rheological model used for a slip event. The peeled strip is modeled by a spring. The failure front is divided into widths b_i, each of them being modeled by a spring in series with an anti-slip pad whose characteristics are represented in the right side of Figure 11.

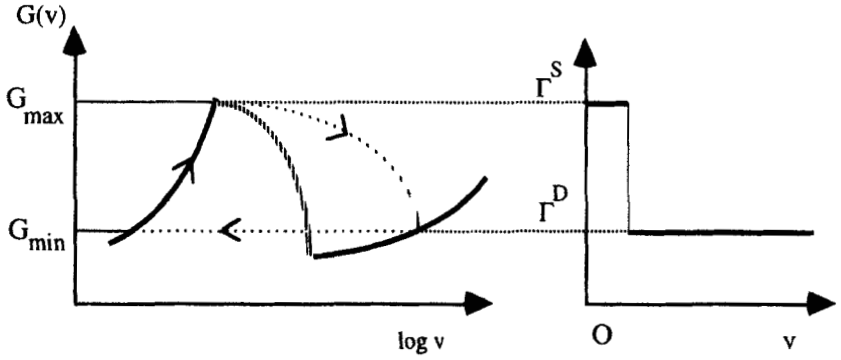

FIGURE 11 Modeling of the $G(v)$ diagram of Figure 1 by a two-level peeling force diagram $\Gamma(v)$. The rupture energy of the interface is much stronger at low velocities than at high velocities. Failure is cohesive in the former case and interfacial in the latter.

assumption that the slip distance Δx_j is negligible with respect to L_0, we have:

$$\Delta F_j = F_b - F_a \approx (Ew/L_0)(1+\varepsilon)(\Delta x_j b_j) \approx (Ew/L_0)(1+\varepsilon)\Delta S_j \qquad (5)$$

This equation is compatible with the linear variation of ΔF_j as a function of ΔS_j shown in Figure 9. The coefficient of proportionality, $(Ew/L_0)(1+\varepsilon)$, is independent of temperature because the temperature variation of E is negligible in the narrow

range investigated here. In fact, we experimentally verified Equation (5) in all slip events without bifurcation (where the front width, b, is determined) as follows. On the one hand, by using the mean slope of the rising curves (as in Fig. 3), we obtain the experimental value of $dF/dL = Ew/L_0$. On the other hand, we can independently measure the amplitude of the force drops and compare it with the slip distance obtained from the macrographs (as in Fig. 5). Knowing the initial parameters in order to evaluate $(1+\varepsilon)$, we always check that the average value of $\Delta F_j/\Delta x_j$ is equal to $dF/dL(1+\varepsilon)$, within a few per cent.

From Equation (5) we can now understand the erratic values of the force drops and the slip cells areas and, thus, the random character of the cell pattern. This equation gives only a relation between ΔF_j, b_j and Δx_j but in no way does it give the absolute values of $\Delta F_j, b_j$ and Δx_j. In other words, the evolution of the system is not deterministic.

If we compare Equations (2) and (5), we obtain:

$$\Gamma_j^S - \Gamma_j^D = (Ew/L_0)(1+\varepsilon)\Delta x_j \tag{6}$$

Recalling the relative constancy of the slip distance, Δx_j, this last equation justifies *a posteriori* the two well-defined energy levels assumption. In other words, this last equation must not be j-dependent whereas Equation (5) strongly depends on the value of the width, b_j, chosen by the system for each slip event.

Dealing with a multi-valued strain energy release function,[1,2] and keeping in mind that, as far as its mechanical equilibrium is concerned, the peeling test geometry belongs to the indifferent kind,[5] it is not surprising that a small perturbation in the peeling system can produce a local unpredictable jump from one to another branch of the $G(v)$ curve.

MICROMECHANICS OF THE STICK-SLIP

1. AFM Observations

We systematically characterized by AFM analysis, as described in a previous paper,[7] different regions of the peeled glass surface identified by optical observations. Actually, except for some cases where delamination between the backing and the polymer sheet occurs at the highest peeling forces (150–250 N/cm), the locus of failure is never far from the glass surface. The peak-to-valley roughness of the peeled substrate does not exceed 2 μm and it is easy, by using AFM, to explore zones as large as $30 \times 30 \mu m^2$.

The inspection of the polymer residue in the adhesive mode region confirms previous facts depicted for peeling at room temperature.[6] The rupture remains heterogeneous but quasi-interfacial. However, the root-mean-square roughness ($\sigma_{RMS} \sim 10-20$nm) is higher for peelings performed in the range 50°C–65°C (Fig. 12) than at room temperature ($\sigma_{RMS} \sim 0.5-1$ nm), a result which indicates that the residual layer thickness increases when the polymer softens.

We now turn to the analysis of the regions where the failure is cohesive. The main new results can be summarized as follows.

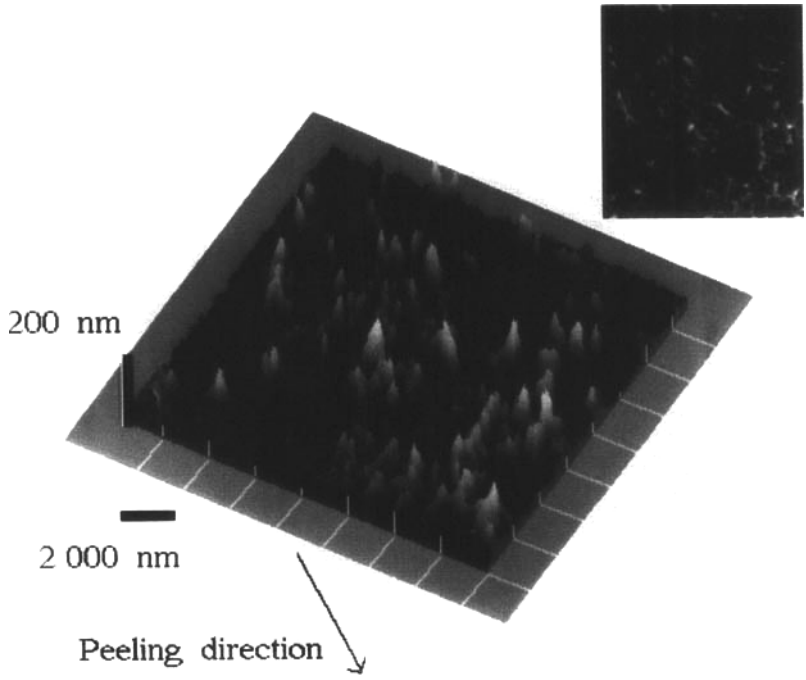

FIGURE 12 AFM image of the glass surface after peeling, recorded in a "slip" region as characterized by optical observations. The peeling conditions are $T = 50°C$ and $V = 0.5$ mm/mn. The insert is a bird's-eye view of the same zone. At this level, the failure appears to be quasi-interfacial. (See Color Plate VII).

- From 40°C to 50°C, we observe large, randomly-distributed polymer residues. They are not connected to each other and their heights range between 0.5 and 2 μm. They are frequently more or less linear-shaped and oriented along the peeling direction.
- From 55°C to 60°C, the polymer residues are more regularly organized as is clearly visible on the optical photograph in Figure 6. They appear much more linear, and *parallel* to each other and to the peeling direction. We interpret them as the reminiscence of the PU walls connecting the peeling strip to the substrate just before the failure was completed. At 60°C these walls are regularly decorated on both sides by arms *perpendicular* to the walls, and therefore parallel to the peeling front, in a periodic dendritic-like pattern. A careful examination of Figure 6 permits one to distinguish them but they are, of course, much better resolved by AFM, as shown in Figure 13. When the walls are sufficiently well separated, the inter-wall region appears covered by holes with dimensions in microns, shown in Figure 14.
- At 65°C, the density of walls is so high that the arms on the edge of two neighbouring walls meet, giving rise to a two-dimensional array which triggers the hole pattern, and the structure appears more regular (Fig. 15). The average dimensions of these holes are determined by the well-defined arm periodicity, λ (about 2μm),

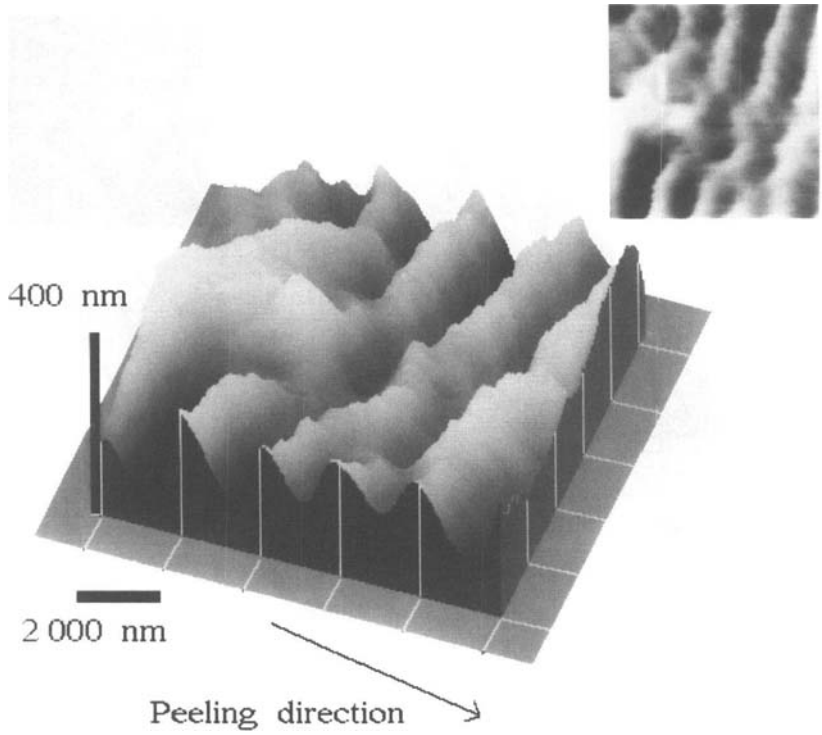

FIGURE 13 AFM image of the glass surface after peeling, recorded in a "stick" region, where the failure is cohesive. The peeling conditions are T = 60°C and V = 0.5 mm/mn. The insert is a bird's-eye view of the same zone. Walls analogous to those visible in Figure 5 are present in this region, but are not shown on this image that puts the emphasis on periodic arms that decorate the edges of the walls perpendicular to them. (See Color Plate VIII).

and the less regular distance between the walls (2–10μm). The height of the walls vary from 0.5 to 2 μm, those of the arms from 30 to 100 nm.

2. DISCUSSION

a) Microscopic coherence length If we accept the natural idea that the observed structures are representative of the distribution of matter just before the passing of the rupture front, we can infer that, as well as at the macroscopic scale there is, at the microscopic one, a continuous transition when the temperature is raised. At low temperatures, when the polymer is tough and when the rupture surface tends towards the interface, the volume involved by the high stress concentration factor is smaller and the flow effects can only produce localized legging[11], or crazes in a more general acceptance of this term. When the temperature is raised, the fall of the viscosity allows flow effects to act at a larger scale and the behavior is more collective. At this level it is, thus, possible to introduce a *microscopic* coherence length

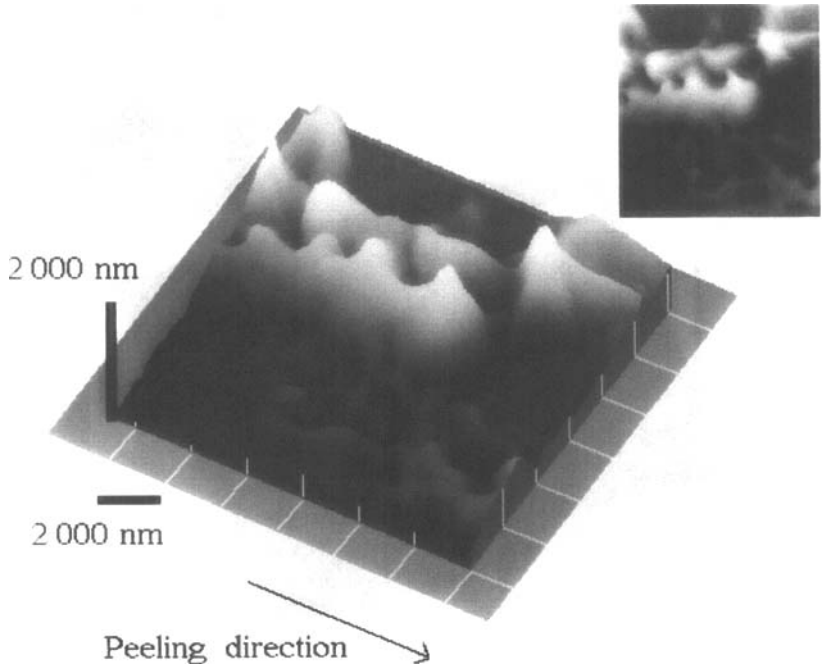

FIGURE 14 Same as Figure 13 with same peeling conditions. In this case, the interwall distance is large and the image is recorded in a region free of walls and arms, which shows a bidimensional array of holes of micronic dimensions. (See Color Plate IX).

(analogous to the macroscopic one), which characterizes the mean distance between the main walls. This behavior parallels those described at the macroscopic level in the preceding section: at lower temperature, where ξ lessens, the system tends to respond to the stress by more localized deformations and the bifurcation is the appropriate answer. A further step to a better understanding of these features would be the study of the evolution of the mean distance between crosslinks with temperature. It is in progress in our laboratory by means of rheological measurements.

b) Crazing and cavitation The perpendicular spatial periodicity, λ, shows that, in order to generate the hole structure described above, it is necessary to accept, as it is generally the case in polymer fracture physics[17], the existence of nucleation and growth of voids before the arrival of the failure front, as was already suspected in earlier experiments on poorly crosslinked polymers[3,18-19]. The nucleation of these voids is favored by the strong negative hydrostatic pressure in that region[14,20-23], and their growth by the lower viscosity. If we apply Gent's criterion[3,20-21] giving the critical triaxial tension for a steady growth of a cavity, $P \approx 5/6\ E$, we find in our case $P \approx 7.5$ MPa. This level is always reached inside the polymer near the failure front during the stick stage ($F \geqslant 100$ N acting on an area $\approx 12 \times 1$ mm^2), particularly at higher temperatures where the crosslinking is reduced, as was mentioned before. This last effect weakens the polymer but the long range deformations occuring in that

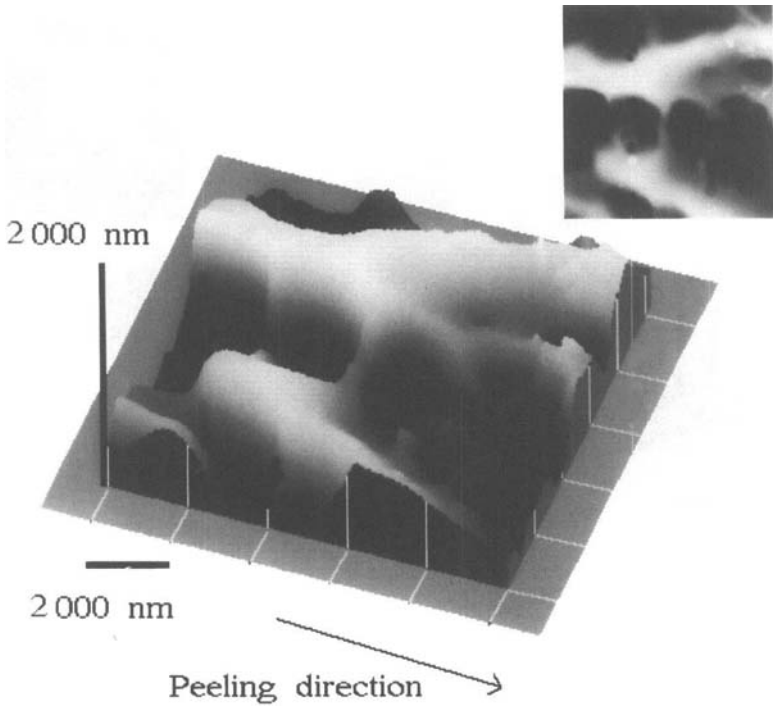

FIGURE 15 Same as Figure 13. Peeling conditions: T = 65°C and V = 0.5 mm/mn. Here, the density of walls is so high that the walls and arms pattern triggers the array of holes. (See Color Plate X).

case considerably increase the dissipative volume, which explains the high peel forces measured in this mode of failure. Withstanding of the peeling forces by the polymer is even enhanced by the geometry of the connecting walls due to the three axial stress effects, and to the strainhardening of the polymeric matter inside the connecting walls[3]. A sketch of our description is proposed in Figure 16. Along the peeling direction (x direction), the void nucleation centers are regularly spaced due to the moving high gradient of the stress distribution ahead of the front. Along the y direction, where the stress is more or less constant, the distribution is not so well determined and only the coalescence of voids may play a role in the alignment of the arms.

Moreover, if we admit the cavitation model, we must take into account the role of the atmospheric pressure in the failure process, when the advancing front gets close to the voids, by setting off the tearing of the connecting arms due to the pressure difference. If we make some calculations using the crude assumption that the maximum critical diameter, d, of the vacuum void is determined by the balance between the inner surface energy, γ (40 mJ/m^2), and the external atmospheric pressure, ΔP, we can write: $4\pi\gamma(d/2)^2 \approx 4/3\pi(d/2)^3\Delta P$, thus we find: $d \approx 6\gamma/\Delta P \sim 2.4$ μm. This evaluation is compatible with the measured periodicity, λ, of about 2 μm. To confirm the validity of this approach, it would be of interest to carryout the same experiments in vacuum,[24] or under higher pressures.[25] This last experiment was

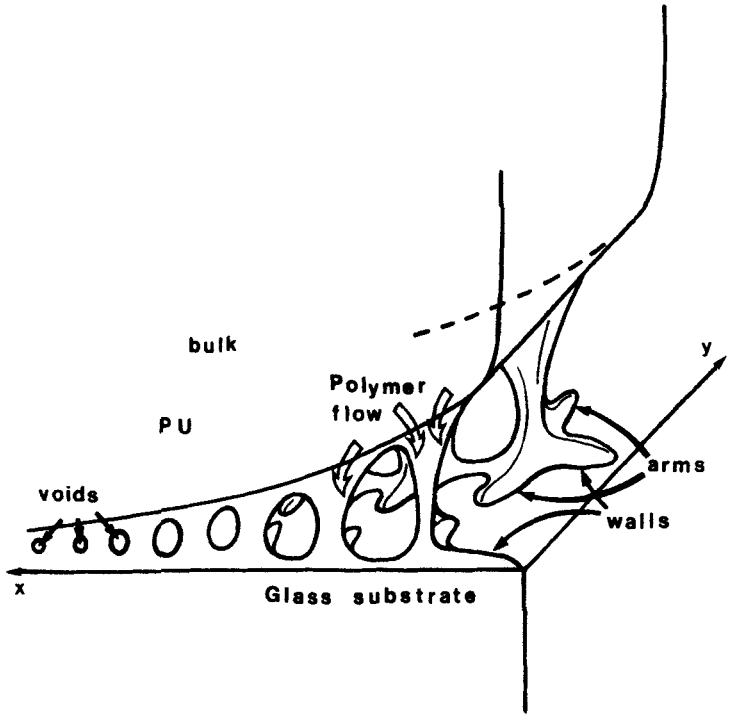

FIGURE 16 Sketch of the proposed repartition of the polymer during the failure process moving from right to left (x axis). As for crazing, the connecting elongating legs or walls are fed from the polymer bulk, which means, here, only from one side of the failure surface. At high temperatures, when the matter can flow over longer distance, walls (and arms) are favored. At lower temperatures, the legging is favored and the coherence length, ζ (parallel to y axis), lessens.

already performed by Gent and Petrich[3] and these authors did not find any difference in the peeling force. That could mean that it does not depend on the exact geometry and repartition of the connecting strands, but much more on their rheological properties at high elongations.

These flow mechanisms explain another effect. The maximum stress concentration is localized near the interface which explains the nucleation of voids there. Moreover, the failure process being attributed to the weakening of the polymer by the void growth, a mechanism in which the flow effects are the dominant ones, we can notice that, in contrast to the classical crazing description, we are here in an *asymmetric* situation of crazing where the glass side cannot feed the elongating craze (or wall) formation. In that sense, the sketch given in Figure 16 differs from the classical image of the symmetrical crazing as illustrated, for example, in Ref. 22, Figure 6. Consequently, the thinner parts of the connecting walls are localized near the interface, and the rupture front is, thus, not allowed to bifurcate into the bulk. On the contrary, the front is always led towards the interface even in such an unstable regime as the stick-slip one.

Finally, we must mention here a marginal – but illustrative – fact, as was already reported for another system.[26] Sometimes when the peeling force, at high temperature, was too high and provoked the delamination of the backing, we tried to cut the polymer with a razor blade in order to force the failure to return near the interface. In fact, it was very difficult to reach the interface using so rough a method. At best, the failure was at several tens of micrometers from the interface. When resuming the experiment, we surprisingly did not observe the expected stick-slip regime, but a true cohesive regime at a constant high peel force, around 2 G_{max}. Now, we can understand this fact. In that case, where the failure initiation is sufficiently far from the interface, *i.e.* further away than the correlation length, ξ, the void creation and the viscous flow generated become symmetrical inside the bulk. The voids continue to act as stress concentrators but, because of the symmetry, drive the failure inside the polymer. The measured force is doubled because the affected dissipative volume ($\sim \xi^3$) is not restricted by the glass side.

CONCLUSION

We have tried in this work to clarify the description of the complex behavior which characterizes the debonding of a peeling test piece in the regime intermediate between interfacial and cohesive. The basic phenomenon is the stick-slip oscillation where the system sequentially jumps from one to the other branch of the $G(v)$ curve.

We have confirmed that the failure is cohesive in the "stick" stage and interfacial, or quasi-interfacial, in the "slip" one. The careful examination of the polymer remaining on the glass substrate during a "stick" stage has revealed complex and regular geometrical shapes of micrometric dimensions that we interpret as resulting from deformation and flow of polymeric matter, as for the crazing mechanism. The same observations lead us to propose the formation of voids near the interface ahead of the failure front.

At the macroscopic scale, the situation can be still more complex because of the possible occurence of bifurcations of the failure front. This causes an erratic force-versus-time recording. In this situation the system is non-deterministic and the relevant approach would be that of the physics of instabilities and non-linear phenomena.

We feel that one of the most important outputs of these observations is the understanding that there is a continuous transition from the "legging" repture (at low temperatures), which appears specifically localized because the flow effects have no time to sustain the imposed stress, to the wall-and-arms rupture (at higher temperatures) which appears specifically collective since the polymer can resist the stress by expending the rupture energy over a much larger space range and flow without breaking the polymeric chains, which is allowed by the uncrosslinking from 50°C. This effect must be studied in relation to the viscoelastic properties of the polymer, especially at very high elongation rate, as we have started in our laboratory.

Of course, these features apply essentially to non-chemically-crosslinked elastomers and, preferably, to strain-hardening materials, but, in every particular case, it is possible to define a pertinent scale where the phenomena discussed in this article

are more or less present. For example, we were able to observe the macroscopic cellular pattern after the peeling of a chemically-crosslinked silicone rubber from glass at a much smaller scale (micron-sized slip cell areas).[27]

Another output is that the rupture surface is naturally directed near the interface, even in the more "liquid" regime at high temperatures because of the *asymmetric* crazing mechanism. On the one hand, this mechanism, in which the three axial effects are enhanced, partly explains the high level of the measured peel force. On the other hand, the voids act as stress concentrators and direct the locus of failure where they are primarily initiated.

This last remark leads us to a very practical conclusion: If your shoes are getting old and the interface between the sole and the inner sole threatens to give up, make a notch in the center of the sole parallel to the interface. To advance in such an induced cohesive regime, the failure needs a much higher peeling force and the shoes will last much longer. One of us tried it. It works!

Acknowledgements

The enthusiastic energy provided by Ms. S. Mocaer, during her initiation to the AFM and mechanical test techniques, is greatly acknowledged.

References

1. A. N. Gent and J. Schultz, *J. Adhesion*, **3**, 281 (1972).
2. D. H. Kaelble, *Colloid Sci.*, **19**, 413 (1964).
3. A. N. Gent and R. P. Petrich, *Proc. Roy. Soc.*, **A310**, 433 (1969).
4. E. H. Andrews and A. J. Kinloch, *Proc. Roy. Soc.*, **A332**, 385 (1973).
5. D. Maugis and M. Barquins, *J. Phys. D: Appl. Phys.*, **11**, 1989 (1978).
6. A. N. Gent, *Le Vide, Les Couches Minces*, suppl. No. 258, 1 (1991).
7. F. Creuzet, G. Ryschenkow and H. Arribart, *J. Adhesion*, **40**, 15 (1992).
8. J. M. Berquier, T. Buffeteau, P. Chartier, B. Desbat and H. Arribart, *Compt. Rend. Acad. Sci. (Paris)*, **315**, 1623 (1992).
9. J. L. Gardon, *J. Appl. Polym. Sci.*, **7**, 625 (1963).
10. D. Maugis and M. Barquins, in *Adhesion* 12, K.W. Allen Ed. (Elsevier Applied Science, London and NewYork, 1988), p. 205.
11. D. W. Aubrey, G. N. Welding and T. Wong, *J. Appl. Polym. Sci.*, **13**, 2193 (1969).
12. D. C. Hong and S. Yue, *Phys. Rev. Lett.*, **74**, 254 (1995).
13. D. Maugis, *J. Mat. Sci.*, **20**, 3041 (1985).
14. D. H. Kaelble, *Trans, Soc. Rheol.*, **15**, 275 (1971).
15. C. Hepburn, in *Polyurethane Elastomers, 2nd. ed.* (Elsevier Applied Science, London and New York, 1992).
16. P. Manneville, in *Dissipative structures and weak turbulence* (Academic Press, New York, 1990).
17. H. H. Kausch, in *Polymer Fracture* (Springer-Verlag, Berlin, Heidelberg, 1987), p. 273.
18. D. H. Kaelble, *Trans. Soc. Rheol.*, **9**, 135 (1965).
19. D. H. Kaelble and R. S. Reylek, *J. Adhesion*, **1**, 124 (1972).
20. A. N. Gent and P. B. Lindley, *Proc. Roy Soc. London*, **A 249**, 195 (1958).
21. A. N. Gent and D. A. Tompkins, *J. Polym. Sci.* A-2, **7**, 1483 (1969). A. N. Gent and C. Wang, *J. Mater. Sci.* **26**, 3392 (1991).
22. A. S. Argon and M. M. Salama, *Phil. Mag.*, **36**, 1217 (1977).
23. R. Schirrer, in *Introduction à la Mécanique des Polyméres*, C. G' sell and J.M. Haudin Eds. (INPL, Vandoeuvre-lès-Nancy, 1995).
24. A. N. Gent, private suggestion (1994).
25. Suggestion given by one of the referees.
26. L. H. Sharpe, *Le Vide, Les Couches Minces*, suppl. No. 272, 237 (1994).
27. G. Ryschenkow, P. Rémy and S. Touraine, *Le Vide, Les Couches Minces*, suppl. No. 272, 90 (1994).